Acta Astronautica 166 (2020) 277–289

Contents lists available at ScienceDirect

Acta Astronautica

journal homepage: www.elsevier.com/locate/actaastro

Research paper

Potential application of X-ray communication in Martian dust storm

Shuang Hang, Xiaobin Tang*, Huan Li, Yunpeng Liu, Junxu Mu, Wei Zhou, Peng Dang, Sheng Lai

Department of Nuclear Science and Technology, Nanjing University of Aeronautics and Astronautics, 29 Yudao St., 210016, Nanjing, China

ARTICLE INFO

Keywords:
Mars communication
X-ray communication
Optical communication
Martian dust storm
Light extinction
Communication performance

ABSTRACT

X-ray communication (XCOM) is an advanced space-communication technology. The high penetration of X-ray enables XCOM to achieve lower signal attenuation than conventional optical communication in Martian dust storm. This study provided a demonstration of this approach based on simulation methods. The transmission properties of X-ray beams in Martian non-dust storm weather were evaluated based on the MCNP5 code. Results demonstrated that the X-ray beam can transmit through a long-distance in Martian atmosphere. Moreover, on the basis of the anomalous diffraction and Mie theory codes, the transmission properties of X-ray and optical links in Martian dust storm were evaluated. Results showed that the dust attenuation of the X-ray links were significantly lower than that of optical links. Moreover, the penetration and communication performance of X-ray links were evaluated and compared with the optical link, considering atmospheric and dust attenuation. Results indicated that XCOM can be used to establish a low-BER communication link between rovers, and from the rover to the orbiter, in Martian dust storm.

1. Introduction

Mars exploration has now become a hot topic for space missions. China has officially approved the Mars mission and plans to launch a Mars probe consist of one orbiter and one rover in 2020 [1,2]. Future landing-exploration missions to Mars have a great demand for communication bandwidth. As a large-capacity communication technology, free-space optical (FSO) communication has one to three orders of magnitude more bandwidth than the radio-frequency (RF) system and is thus suitable for Mars exploration missions [3,4]. Moreover, optical communication can also offer size, weight, and power advantages over RF systems due to its short wavelength. In Mars missions, optical links can not only provide the use of high-performance scientific instruments but also support real time high-resolution video in future manned missions [5]. However, conventional optical links, also known as laser communication links, will be severely attenuated or even interrupted by the frequent dust storms in Mars [6–8].

X-ray communication (XCOM) is a special type of wireless optical communication, which also has the advantage of low divergence and high bandwidth [9]. XCOM uses modulated X-ray beams as a carrier for data transmission and is considered to be the next-generation aerospace communications technology [10]. Researchers at NASA Goddard Spaceflight Center has developed a modulated X-ray source with the switching time of nanoseconds and a communication control module called NavCube. Based on this system, NASA will conduct a 50 m XCOM demonstration on the International Space Station in 2019 [11]. Researchers at the Chinese Academy of Sciences have developed grid-controlled X-ray sources and further realized the X-ray based data transmission with a data rate of 240 kbps [12]. Researchers at Nanjing University of Aeronautics and Astronautics have proposed a new X-ray modulation method based on laser-to-X-ray conversion, which can increase the modulation rate up to 100 Mbps [13]. Researchers at Saint Petersburg Electrotechnical University have built their XCOM prototype based on the photo-X-ray tube and experimentally determined that this XCOM scheme can provide a transmission rate up to 10 Mbps [14].

XCOM can be used to establish a communication link between a re-entry vehicle and a satellite. In this process, XCOM link can avoid communication blackout due to its high plasma penetration [15,16]. Based on the strong penetration performance of X-rays, we expect that XCOM links may be immune from dust disturbance. In this study, we propose the use of XCOM to mitigate the extinction effect of dust and to achieve high-speed data transmission during Martian dust storms among spacecrafts on Mars. The XCOM among spacecrafts is shown in Fig. 1. Two communication scenarios are considered: the communication link between the rover and the Mars orbiter and the short-distance communication link between two Mars rovers.

In this study, the theoretical analysis method is used to evaluate the performance of XCOM links in Martian dust storms. Moreover, the performance of optical links is also calculated under the same dust storm conditions, and the results are used as indicators of the signal

* Corresponding author.
E-mail address: tangxiaobin@nuaa.edu.cn (X. Tang).

https://doi.org/10.1016/j.actaastro.2019.10.025
Received 13 January 2019; Received in revised form 27 September 2019; Accepted 8 October 2019
Available online 14 October 2019

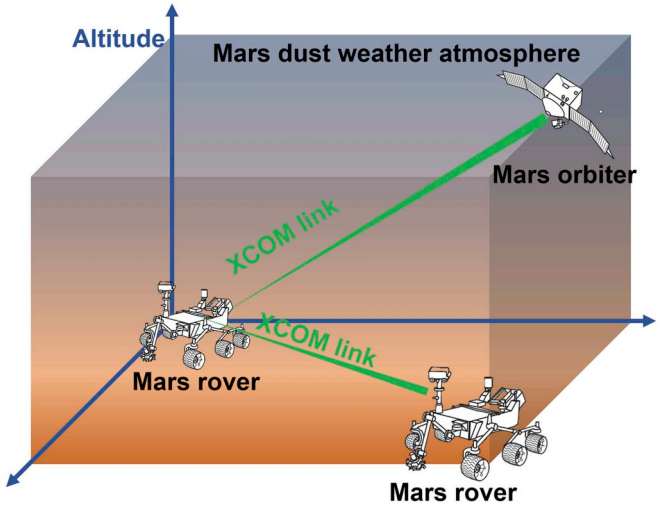

Fig. 1. Schematic of XCOM in Martian dust storm weather.

attenuation caused by dust storms. In the following sections, the atmospheric attenuation and dust extinction processes of X-ray are simulated. Based on the simulation results and the communication model, the performance of the XCOM link under different communication scenarios are obtained.

1.1. Martian dust storm climate

Global and large-regional dust storms represent an important component of the main Martian climate cycles [17,18]. During the Martian dust storm season, suspended dust is widely present in the atmosphere; the global distribution of dust mass mixing ratio is shown in Fig. 2 [19–22]. In this study, four locations were selected for discussion: Northeast Syrtis, Jezero Crater, Columbia Hills, and a large dust storm center. The first three were the three candidate landing sites of the NASA Mars 2020 project [23].

The parameters of dust particles and atmosphere at these locations are shown in Fig. 3, in which the radius of the Martian dust particle can be described by a bimodal size distribution (Fig. 3(a)) [24]; each of the two peaks can be determined by

$$n(r) = (1/r\sigma_g \sqrt[2]{2\pi})\exp(-(\ln r - \ln r_g)^2 / 2\ln^2\sigma_g), \quad (1)$$

where, $n(r)$ represents the single peak of the bimodal size distribution, r is the radius of dust grain, and the coefficients r_g and σ_g can be obtained by

$$r_{eff} = r_g \exp(2.5 \times \ln^2\sigma_g), \quad (2)$$

$$v_{eff} = \exp(\ln^2\sigma_g) - 1, \quad (3)$$

where r_{eff} and v_{eff} are the effective radius and variance of the dust particle. The number ratio γ of dust between small and big modes as a function of the altitude is shown in Fig. 3(b). On the bases of the Mars climate database and the bimodal size distribution, the vertical distribution of dust number density was obtained (Fig. 3(c)). Moreover, the curves of the Martian atmosphere density at four selected Mars locations as a function of altitude are shown in Fig. 3(d) [25–27].

2. XCOM under clear sky condition

2.1. Simulation method

In non-dust storm weather, the absorption of the Martian atmosphere is the main factor, leading to the attenuation of the X-ray link. Unlike optical photons, the attenuation of X-ray photons in the atmosphere is essential. Therefore, the evaluation of atmospheric attenuation in different XCOM scenarios is needed. In this study, an X-ray transmission coefficient evaluation was performed based on the Monte Carlo particle transport program MCNP5 [28]. The Martian atmosphere was modeled based on the data in Fig. 3(d). The calculation error of all results was less than 0.1%.

2.2. Results and discussions

XCOM links from the rover to the orbiter over four selected locations were considered. The transmission coefficients of X-ray links with different energy as a function of attitude are shown in Fig. 4. Results indicated that most of the lost X-ray photons deposit their energy in the atmosphere below 20 km along the propagation path. Above the Columbia Hills, X-ray attenuation was severe due to the high atmosphere density. The 30 keV X-ray beam had a transmission coefficient of 0.07%, and the transmission coefficient increased with increased X-ray energy. When the link energy reached 200 keV, a transmission coefficient of 7% can be achieved. With increased X-ray energy to 800 keV, the transmission coefficient can reach 22%. The 200 keV X-ray links can provide more than 10% transmission at three other locations.

The transmission coefficients of X-ray links between two rovers on Martian surface with different communication distances from 50 m to 2 km were evaluated. Results are shown in Fig. 5. At Columbia Hills, the 2 km X-ray link with energy up to 30 keV can achieve a transmission coefficient higher than 24%, whereas the X-ray link with energy up to 30 keV can provide transmittance more than 30% at the three other locations due to lower atmosphere density. Results of this Monte Carlo

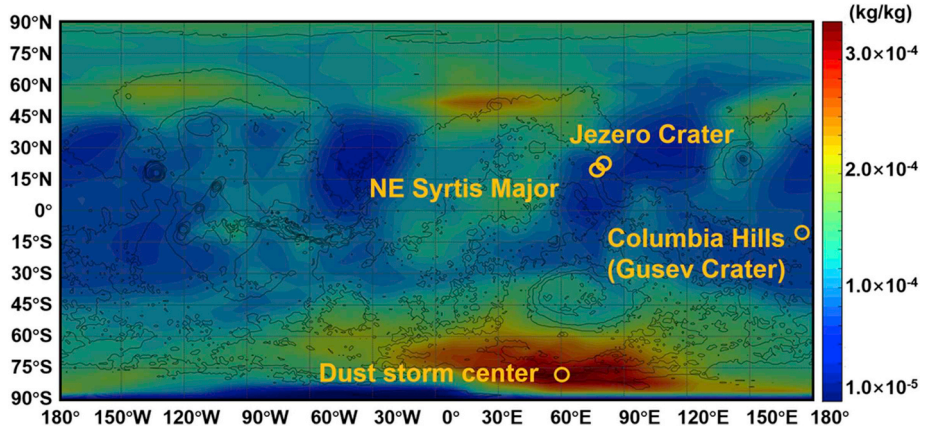

Fig. 2. Global map of dust mass mixing ratio with dust storm maximum solar scenario.

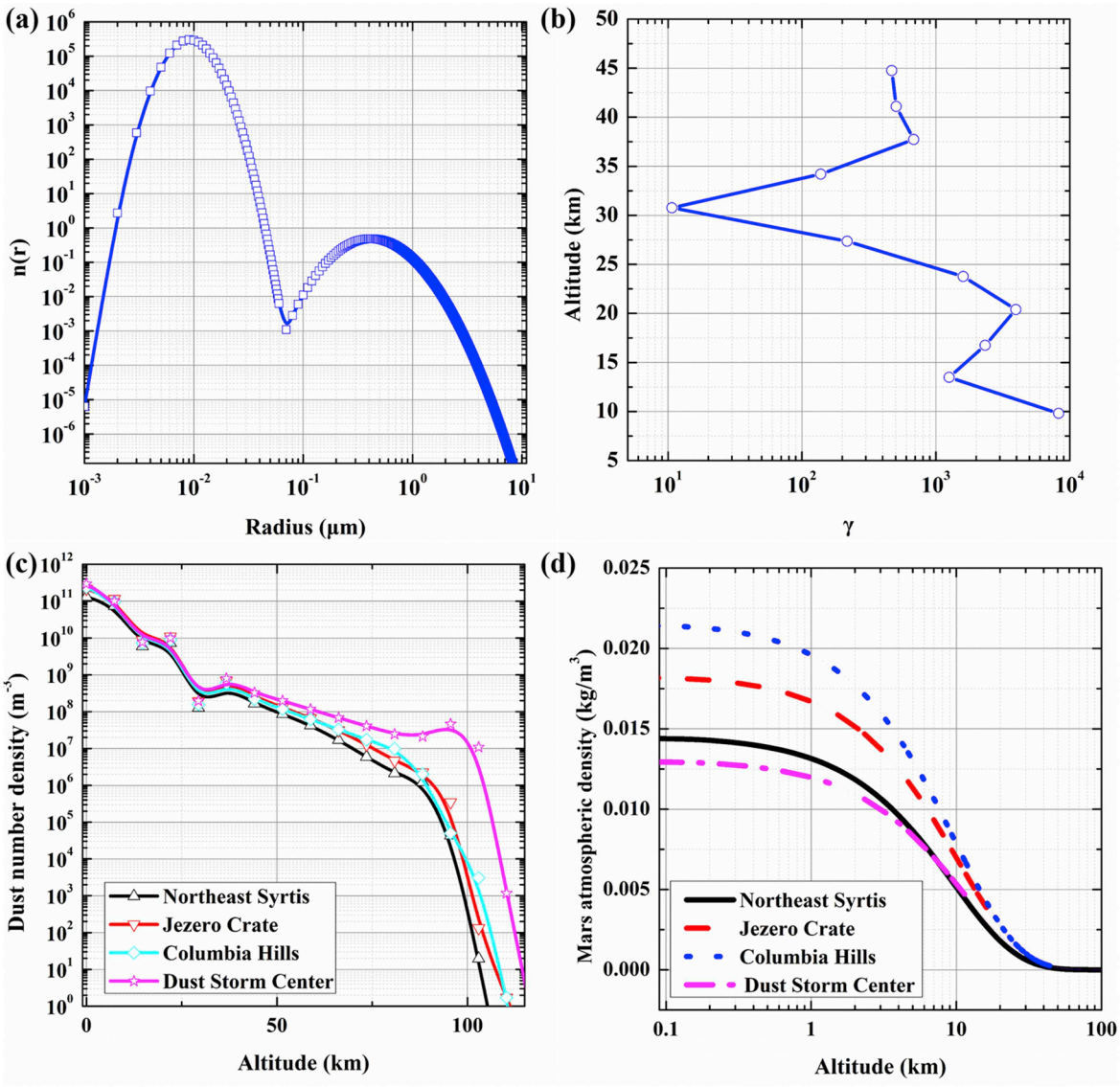

Fig. 3. (a) Radius distribution of Martian dust particles; (b) Population ratio between small and big modes; (c) Vertical profile of dust number density; (d) Vertical profile of the Mars atmosphere density.

simulation showed that under clear sky condition, X-ray beams can realize long-distance transmission in the Martian atmosphere without high-energy requirement. Furthermore, the X-ray beam with energy above 30 keV can be used to build the 2 km link between the rovers, and X-ray beams with energies above 200 keV can be used to build an up-link from the rover to the orbiter.

3. XCOM under dust storm condition

3.1. Simulation method for dust extinction

The impact of dust storm on communication links is caused by the extinction effect of dust particles. As shown in Fig. 6, the extinction effect includes scattering and absorption. In this study, the extinction process of X-ray photons and optical photons was simulated by the General Geometry Anomalous Diffraction Theory (GGADT) [29] and Mie scattering code, respectively [30]. GGADT is an open-source FORTRAN suite that can be used to simulate the collision process between X-ray photons and dust particles. For optical photons, the extinction process was simulated by the Mie scattering theory.

The cross-sections of scattering Q_{sca}, absorption Q_{abs}, and extinction Q_{ext} can be obtained by the simulation. Then, the intensity of the light beam after passing through the dust storm can be expressed by Ref. [31].

$$I = I_0 \exp\left(-\int_0^1 \int_0^\infty \pi r^2 Q_{ext} \rho N(r) dr dl\right), \tag{4}$$

where I_0 is the incident light intensity; r is the dust particle radius; l is the distance of transmission; $N(r)$ is the radius distribution of dust particles; ρ is the number density of dust particles.

During a Martian dust storm, the pulse signal may be broadened and delayed due to multipath effects in the high dust density area. The pulse delay time Δt caused by the multipath effect can be expressed by Equation (5), and the pulse response function P_s can be obtained by Equation (6) [32].

$$\Delta t = (z/c) \times \{0.3z/\omega\tau\theta_0^2[(2.25 \times \omega\tau\theta^2 + 1)^{3/2} - 1] - 1\}, \tag{5}$$

$$P_s(t) = (t/\Delta t^2)\exp(-t/\Delta t), \tag{6}$$

where z is the transmission distance; c is the speed of light; ω is the scattering albedo; τ is the optical thickness; and θ is the scattering angle.

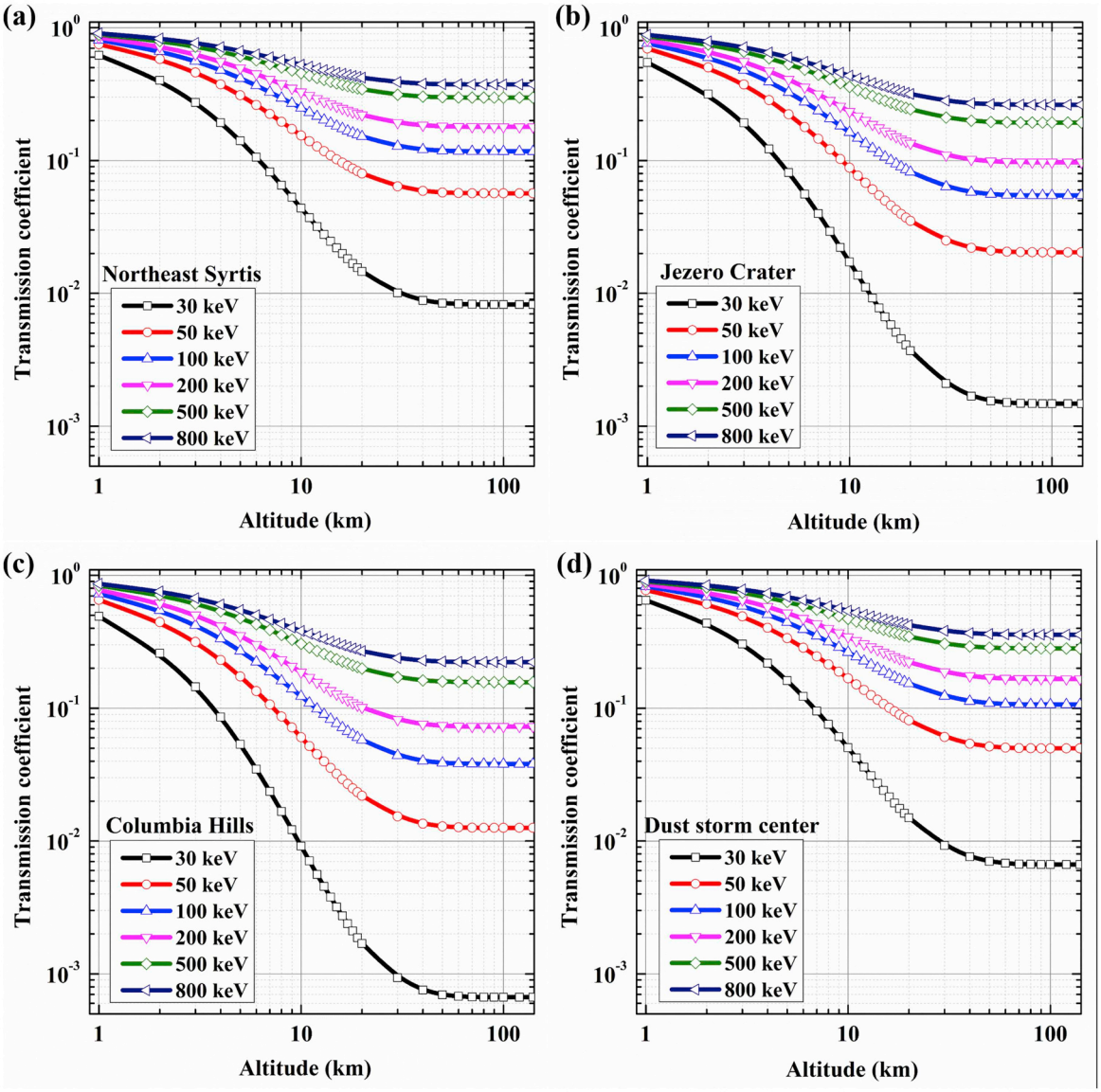

Fig. 4. Mars atmospheric transmission coefficients of the X-ray links from the rover to the orbiter at (a) Northeast Syrtis; (b) Jezero Crater; (c) Columbia Hills; (d) Dust storm center.

3.2. Cross-sections of Martian dust extinction

The absorption, scattering, and extinction cross-sections of photons by dust particles as a function of photon energy are shown in Fig. 7. The energy of X-ray photons was from 100 eV to 20 keV. The optical band included infrared, visible light, and ultraviolet. Fig. 7(a) and (b) were the results of small and big modes of dust in a Martian dust storm, respectively. With increased X-ray energy, the extinction cross-section decreased rapidly, indicating that the extinction of Mars dust particles on high-energy X-ray is extremely weak.

The normalized differential scattering cross-sections of different energy photons were calculated to illustrate the scattering angle distribution of scattered photons. Fig. 8(a) and (b) were the results of small and big modes dust, respectively. This figure showed that the scattering angle of optical photons is considerably larger than that of X-ray. The scattering angle gradually decreased with increased optical photon energy. However, the X-ray scattering angle was extremely small, and the scattered X-ray photons can almost maintain its initial path.

The differential cross-sections of X-ray photons with different energies are shown in Fig. 9. The X-ray scattering cross-section of big mode dust was considerably larger than that of small mode dust, which means that the scattering of X-ray by big mode dust particles is the main factor leading to X-ray dust extinction. Moreover, the X-ray scattering angle was smaller than 2 arcseconds, which means that the scattered X-ray photons can still be received by the detector with a receiving area of 0.05 m^{-2}, after passing through a distance of 13 km.

3.3. Impact of dust storm on communication links

Based on the cross-sections obtained in the previous section and taking the dust storm center location as an example, the transmission coefficient of the communication link was calculated by considering only the dust extinction effect (Fig. 10). Results showed that the dust attenuation of the X-ray link was considerably lower than that of optical link. As shown in Fig. 10(a), in the scenario of 2 km communication between rovers, the transmission coefficient of the optical link was less than 50%, whereas X-ray links of energies above 5 keV can transmit 2 km without obvious attenuation. The transmittance results of communication from the rover to the orbiter is shown in Fig. 10(b). At an altitude of 10 km, the optical link transmission was reduced to

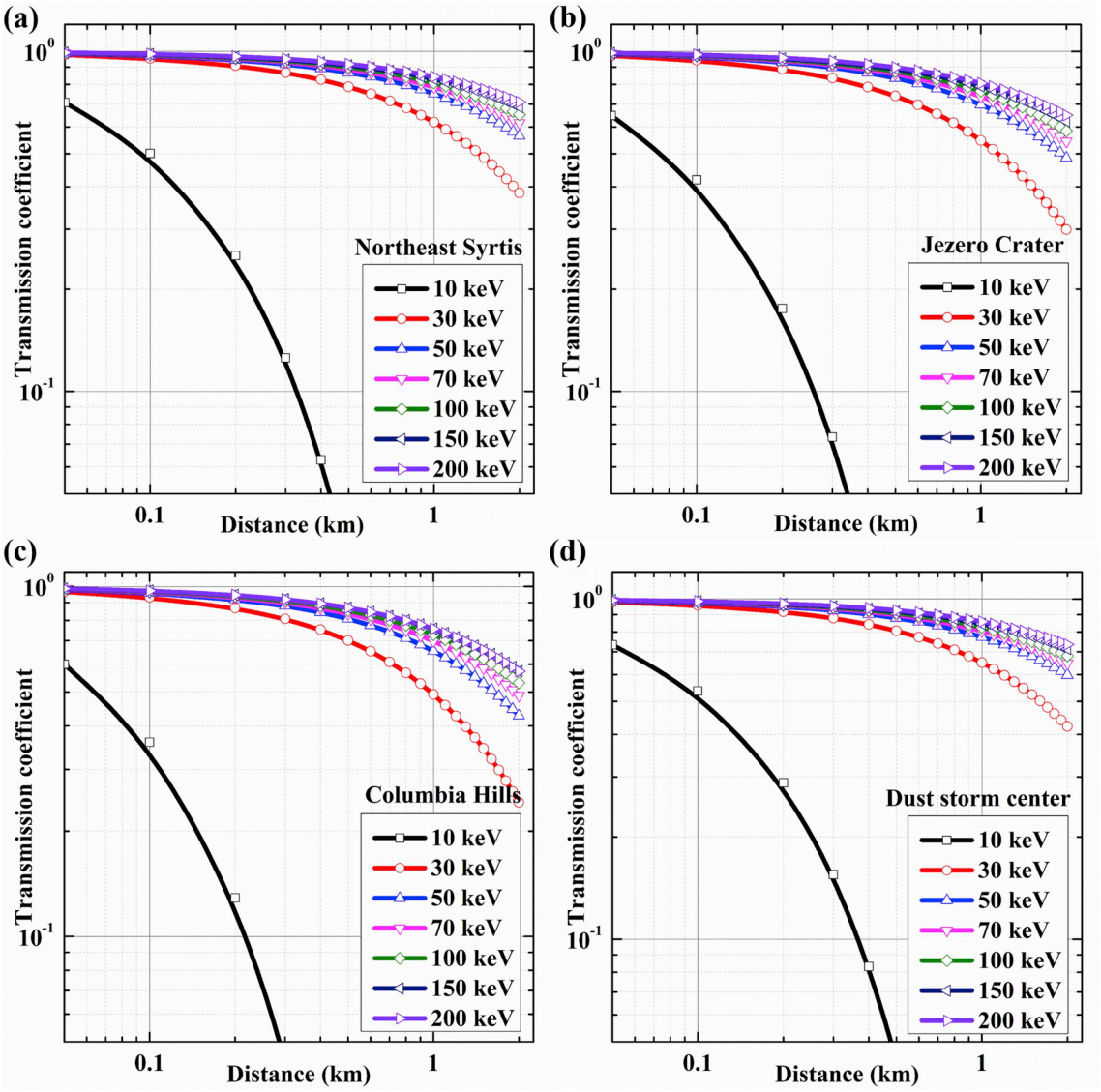

Fig. 5. Mars atmospheric transmission coefficients of the X-ray links between the rovers at (a) Northeast Syrtis; (b) Jezero Crater; (c) Columbia Hills; (d) Dust storm center.

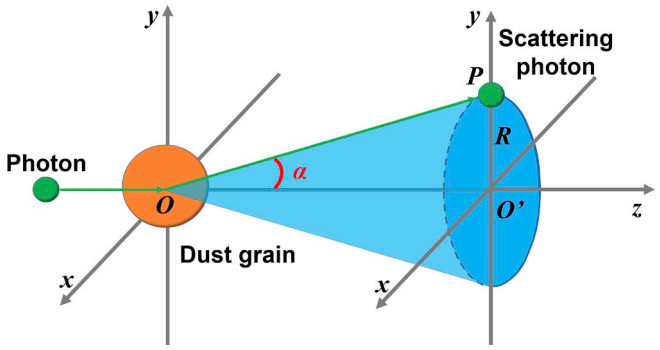

Fig. 6. Schematic of extinction by dust particle.

approximately 0.1. With increased altitude to 140 km, the transmittance of the optical link was reduced to less than 1.5×10^{-8}. Moreover, the X-ray link transmission increased with increased energy. X-ray links with energies above 20 keV would almost be unaffected by a dust storm.

Normalized pulse response functions with transmission distances of 0.5, 1, 5, and 10 km were calculated. The results of optical and X-ray links are shown in Fig. 11(a) and (b), respectively. This figure showed that the pulse delay and the broaden value increased with increased transmission distance. When the transmission distance is 10 km, the broadening and delay time of the optical pulse was several microseconds, whereas the X-ray pulse exhibited a broadening and delay time of less than 1 ps. The calculation results of transmittance and pulse response function showed that the intensity and temporal characteristics of X-ray pulse signals were less affected by dust storm compared with optical pulses.

3.4. Signal attenuation in Martian dust storm

The attenuation of X-ray and optical links is dominated by the absorption effect of the atmosphere and the extinction effect of dust. Considering the atmospheric and dust storm attenuation, the transmission curves of the optical link and the X-ray link were calculated. Transmission curves of the communication links from the rover to the orbiter during the dust storm are shown in Fig. 12. Results showed that the transmission performance of the X-ray link is better than that of optical links. During the dust storm, at an altitude of 140 km, the

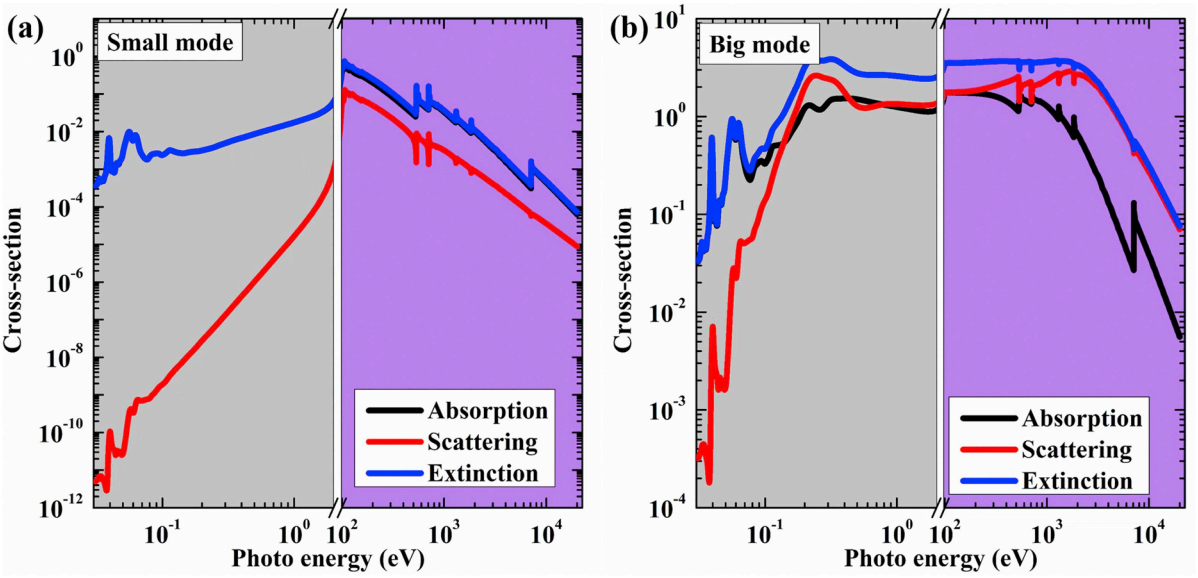

Fig. 7. Extinction, scattering, and absorption coefficients of different energy photons (a) by small mode dust; (b) by big mode dust.

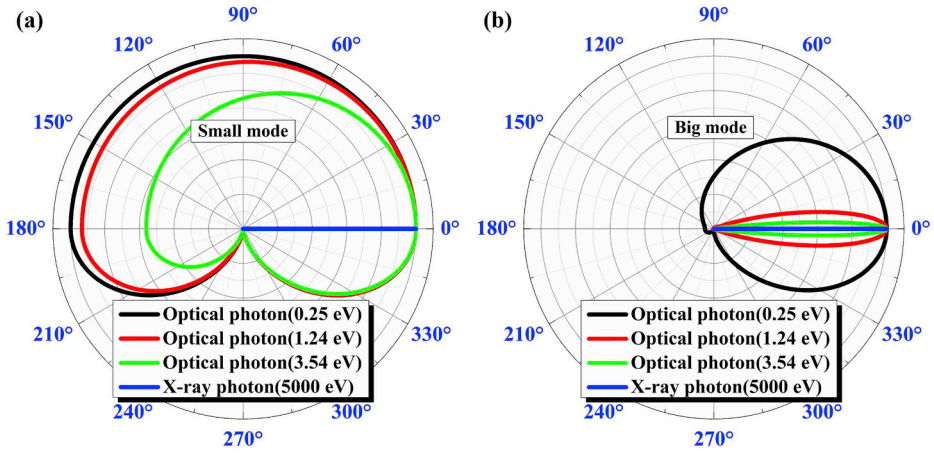

Fig. 8. Normalized differential cross-sections of different energy photons (a) by small mode dust; (b) by big mode dust.

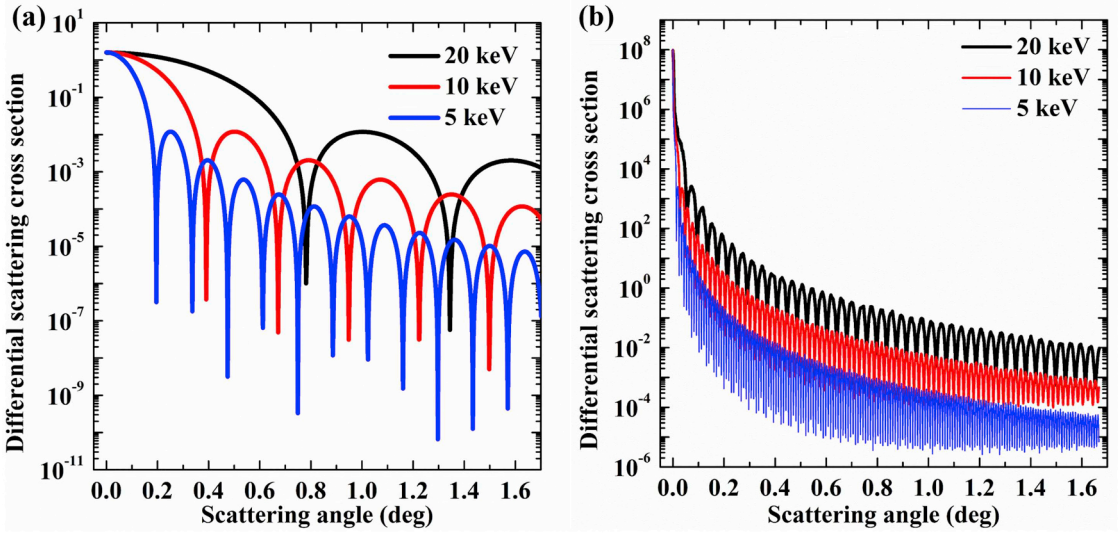

Fig. 9. Differential cross-sections of X-ray photons with different energies (a) by small mode dust; (b) by big mode dust.

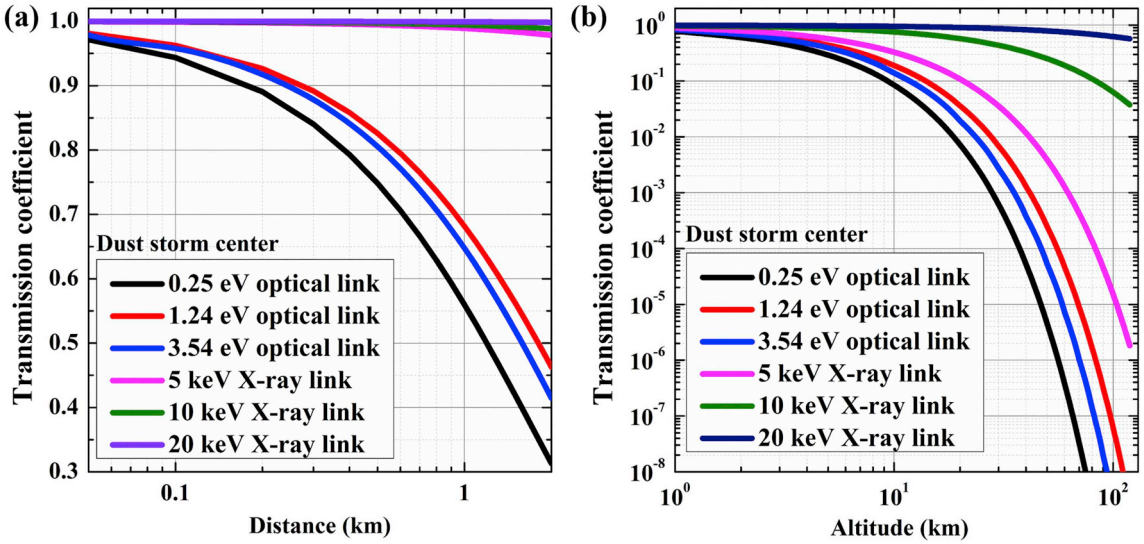

Fig. 10. Transmission coefficients of (a) the communication links between the rovers; (b) the communication links from the rover to the orbiter.

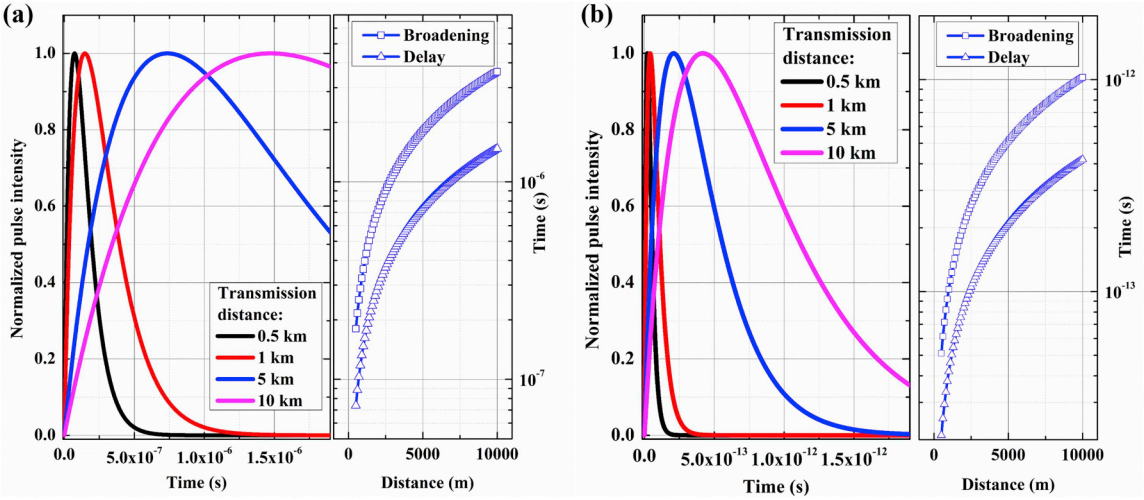

Fig. 11. Normalized pulse response functions of (a) optical links and (b) X-ray links.

transmission coefficient of the 200 keV X-ray link was greater than 7%, and the transmittance of the optical link was lower than 1.5×10^{-8}.

XCOM links from the rover to the orbiter could provide better transmission performance, during the dust storm. However, this result was obtained under the condition that the elevation angle was 90°. When the elevation angle is less than 90°, the slant path of XCOM link will result in a decrease in transmission performance. For this reason, transmission coefficients of XCOM links with different elevation angles were also evaluated. The results of XCOM links with different energies are shown in Fig. 13. The 200 keV XCOM links with elevation angles of 30° and 10° can provide transmission coefficients of 2.763% and 0.003%, respectively. The increase of X-ray energy can significantly improve the penetration of the XCOM link. When the elevation angles are 30° and 10°, transmission coefficients of the 1 MeV X-ray link are 15.74% and 0.49%, respectively.

The transmission curves of the 2 km communication links between the rovers during the dust storm are shown in Fig. 14. Results showed that the transmission performances of X-ray and optical links were close, with the X-ray links performing slightly better. However, at four different Mars locations, the transmission coefficients of 50%–75% can be achieved by the 200 keV X-ray link, which is better than an optical link.

4. Link performance evaluation

4.1. Evaluation method

In this section, the XCOM and optical links were modeled based on the intensity modulation/direct detection communication system. A modulated X-ray source and a high-time-resolution scintillation detector [33] are employed as the transmitter and receiver of the XCOM system. The scintillation detector is coupled by a lutetium-yttrium oxyorthosilicate (LYSO) crystal [34] and an avalanche photodiode (APD). The nested X-ray focusing optics are employed as the transmitting and receiving antennas of the XCOM system [35]. The FSO system consists of a modulated laser diode, an APD and optical antennas [36]. In addition, the acquisition pointing and tracking (APT) system is required to keep both ends of the XCOM and FSO system aligned. The communication performance was evaluated by calculating the signal-to-noise ratio (SNR) and bit error ratio (BER), based on the communication system model. SNR is the ratio of the received signal strength over the noise strength in the frequency range of the operation. BER is the number of bit errors divided by the number of transferred bits during a particular time arrival. In this study, the atmospheric attenuation, dust attenuation, and beam divergence of the links were calculated. The receiving power P_R can be determined by

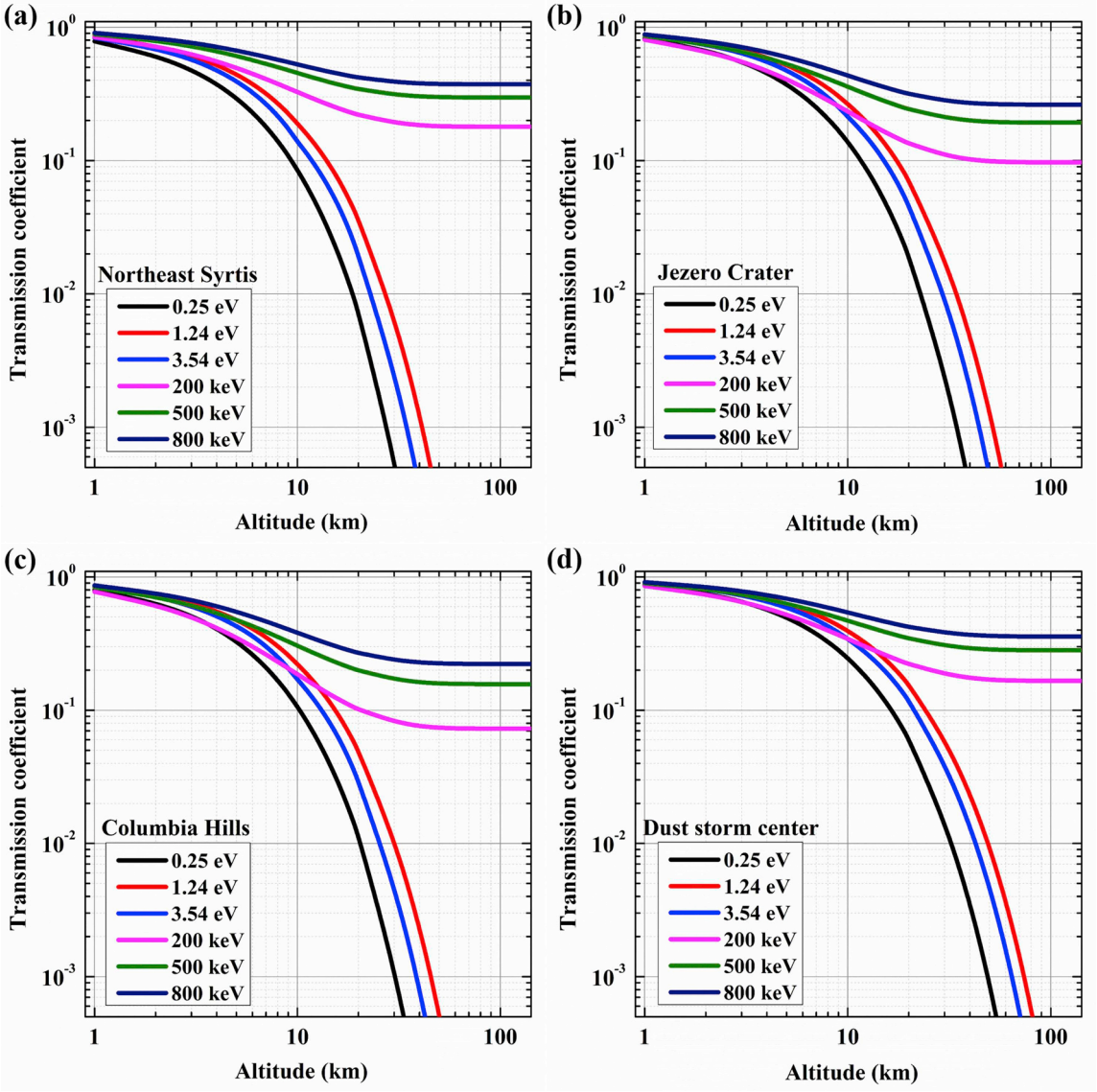

Fig. 12. Transmission coefficients of the communication links from the rover to the orbiter during the dust storm at (a) Northeast Syrtis; (b) Jezero Crater; (c) Columbia Hills; (d) Dust storm center.

$$P_R = A_R P_T C_T \eta_c^2 / \pi \theta_d^2 l^2, \tag{7}$$

where, A_R is the receiving area; P_T is the transmitting power; C_T is transmission coefficient; η_c is the focusing efficiency; θ_d represents the beam divergence; and l is the transmission distance. The SNR of X-ray and optical links can then be determined by (8) and (9), respectively [37].

$$SNR = (B/R) \times (MY_s \eta q P_R / E_s h\nu)^2 / ((MY_s \eta q F_B / E_s)^2 + 2qM^2\, BFI_d + 4KTB/R_L) \tag{8}$$

$$SNR = (B/R) \times (M\eta q P_R / h\nu)^2 / (2qM^2 BFI_d + 4KTB/R_L), \tag{9}$$

where, B is the bandwidth; R is the bit rate; M is the gain of APD; Y_s represents the photon yield of LYSO crystal; E_s is the energy of incident X-ray photon; η is the detection efficiency; F is the excess noise factor; R_L is the impedance of detector; ν is the carrier frequency; I_d is the average dark current; T is noise temperature; q is electron charge; h is Planck constant and k is the Boltzmann constant. F_B is the flux of background X-ray photon and was set to $50\,m^{-2}\,s^{-1}$ in the Martian environment [38]. In order to highlight the dust attenuation of the optical link, background noise of the FSO system was not considered. The APD used in this simulation is Hamamatsu Photonics Si-APD S3884 [39]. The parameters of XCOM and FSO systems can be determined by Table 1.

According to the SNR value, the BER of XCOM system with on–off keying (OOK) and pulse position modulation (PPM) method can then be obtained by Ref. [37].

$$BER_{OOK} = 0.5 \times \mathrm{erfc}(\sqrt{SNR}/2\sqrt{2}), \tag{10}$$

$$BER_{PPM} = 0.5 \times \mathrm{erfc}(\sqrt{(L/2) \times SNR \times \log_2 L}/2\sqrt{2}), \tag{11}$$

where, L is the modulation level and was set to 4 in this calculation.

4.2. Results and discussions

The SNR value of optical and X-ray links in Mars surface-to-surface and surface-to-orbiter scenarios at the dust storm center were calculated, and the BER performance of the OOK and PPM modulated links were then obtained based on the SNR results. For the communication links between the rovers, transmitting power of the XCOM and optical links were set to 61 mW and 1.5 mW, respectively. The SNR and BER

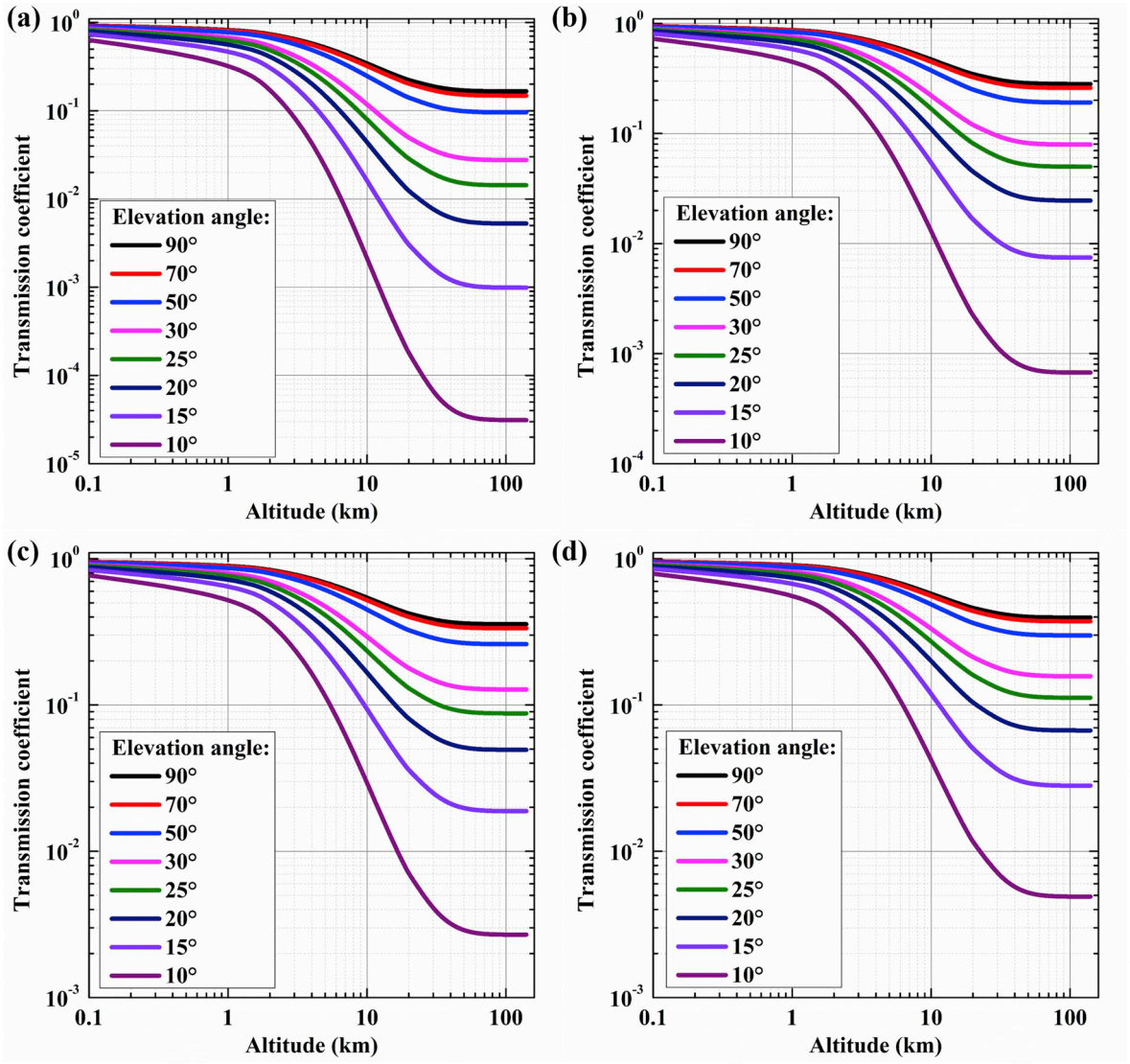

Fig. 13. Transmission coefficients of (a) 200 keV; (b) 500 keV; (c) 800 keV; and (d) 1 MeV XCOM links from the rover to the orbiter with varying elevation angles.

value as a function of the communication distance are shown in Fig. 15. Results showed that in order to achieve similar communication performance, X-ray links require more transmitting power than optical links. This is because the single photon energy of X-ray is much higher than that of laser. As shown in Fig. 15(b), for the same SNR conditions, PPM-modulated links can provide lower BER value than OOK-modulated links. Moreover, on Martian surface, the 61 mW X-ray link and 1.5 mW optical link enable the BER value to be less than 10^{-6}.

For the communication link from rover to orbiter, transmitting power of the XCOM and optical links were set to 3 mW. Results showed that the laser link can be considered completely interrupted, and the SNR performance of X-ray link was much better than that of the optical link (Fig. 16). As shown in Fig. 16(b), the optical link always exhibits a high BER at an altitude more than 60 km, which indicates that the optical link from rover to orbiter interrupt in Martian dust storm. However, X-ray links can provide a good performance under the same condition, which demonstrates the effectiveness of XCOM in Martian dust storms.

The minimum transmitting power required to achieve the BER less than 10^{-6} as a function of the elevation angle were calculated, and the results of the X-ray links with energies of 200 keV, 500 keV, 800 keV and 1 MeV are shown in Fig. 17. In order to achieve the low-BER XCOM, the minimum transmitting power requirement increases significantly as the elevation angle decreases. When the elevation angle is reduced from 20° to 10°, the transmitting power requirement is increased by two orders of magnitude. Obviously, improving X-ray energy can reduce the transmitting power requirement of XCOM link. 1 MeV X-ray link with transmitting power of 18.3 mW can realize low-BER XCOM from rover to orbiter at the elevation angle of 20°.When elevation angle is 30°, the transmitting power of 3.6 mW is sufficient.

5. Conclusions

As a special wireless optical communication technology, XCOM is expected to overcome the interference of Martian dust storm on communication signals. This study preliminarily demonstrated this approach via the simulation method. The Monte Carlo method was used to simulate the propagation of X-ray beams in non-dust storm weather, and the transmittance of different X-ray energies was obtained. The results showed that X-ray beams have the ability to propagate long-distances in the Martian atmosphere. Moreover, the dust extinction processes of laser and X-ray were simulated based on GGADT and Mie scattering theory, and detailed cross-section parameters were obtained. According to these parameters, the transmittance and temporal characteristics of the optical and X-ray links were evaluated. Results indicated that XCOM can resist the interference of Martian dust storms.

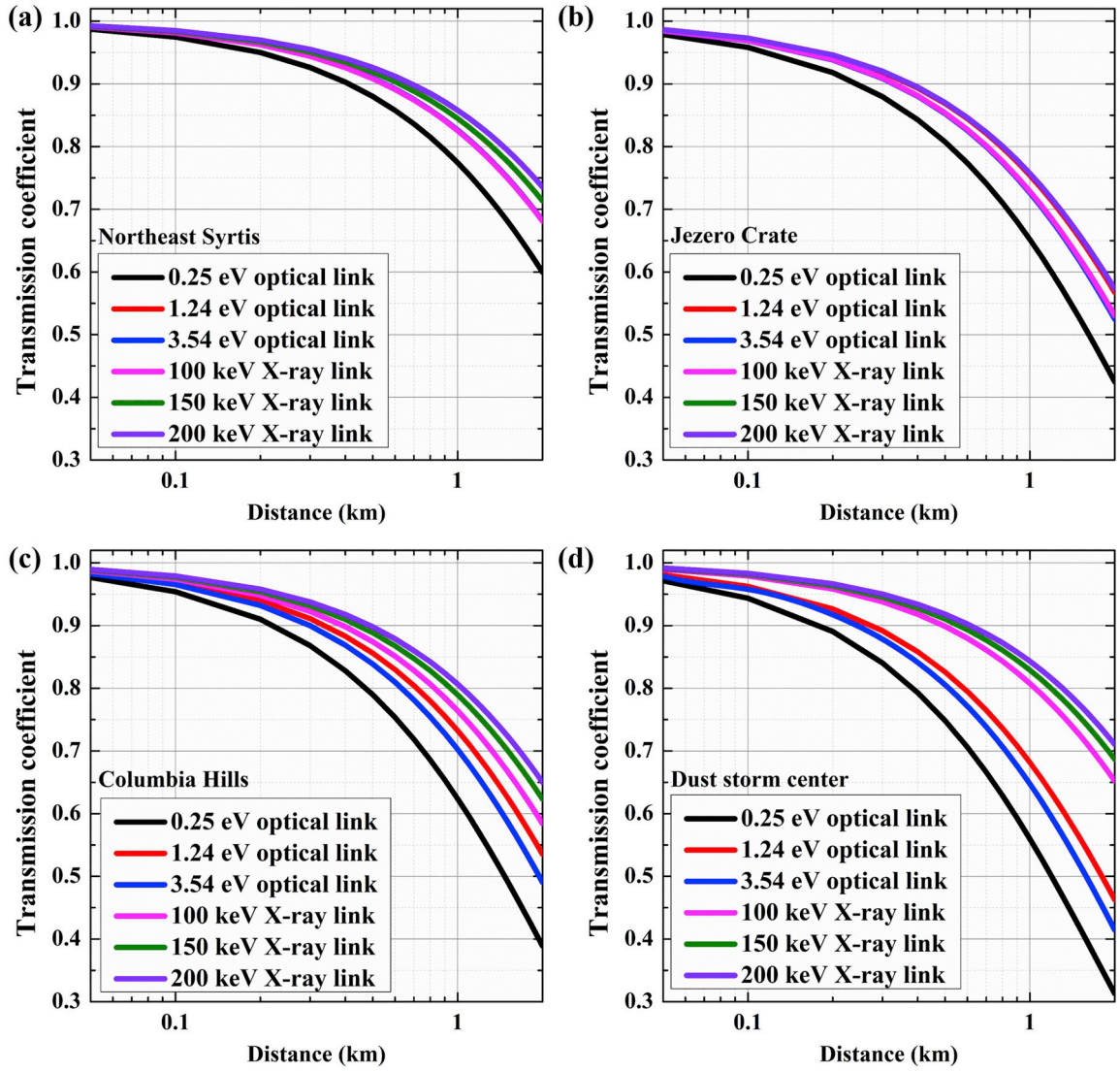

Fig. 14. Transmission coefficients of the communication links between the rovers during the dust storm at (a) Northeast Syrtis; (b) Jezero Crater; (c) Columbia Hills; (d) Dust storm center.

Table 1
Parameters for link performance evaluation.

Parameters	XCOM system	FSO system
Photon energy E_s	200 keV	1.24 eV
Bit rate R	100 Mbps	100 Mbps
Light yield of LYSO Y_s	26300 ph/MeV	–
Gain of APD M	100	100
Quantum efficiency of APD η	75%	75%
Bandwidth of APD B	400 MHz	400 MHz
Dark current of APD I_d	5 nA	5 nA
Focusing efficiency η_c	70%	100%
Receiving area A_R	0.05 m^2	0.05 m^2
Divergence θ_d of surface-to-surface link	10 mrad	10 mrad
Divergence θ_d of surface-to-orbiter link	10 μrad	10 μrad

Furthermore, the communication performance of the optical and X-ray links during a Martian dust storm weather was evaluated by calculating the SNR and BER of the communication links. The results demonstrated that XCOM system can be employed to establish Mars surface-to-surface and surface-to-orbiter links during dust storms. The 61 mW surface-to-surface XCOM link and 3.6 mW surface-to-orbiter XCOM link with elevation angle greater than 30° can achieve the bit rate of 100 Mbps and the BER less than 10^{-6}.

XCOM has advantages of size, weight, power and bandwidth over RF systems and has advantages over FSO systems in anti-dust attenuation. However, it should be pointed out that the XCOM system also has some limitations. In the Martian area with dense atmosphere, the strong atmospheric absorption effect of the X-rays will result in a high transmit power requirement for the XCOM system. Furthermore, the power consumption of XCOM systems will be higher than other communication systems, due to the current immature XCOM devices. Moreover, efficient APT systems are needed to keep both ends of XCOM system alignment. X-ray links with low divergence will challenge current APT technology and increase the difficulty of establishing a communication link. In addition, high power X-ray transmitting may increase the risk of radiation damage. Modulation techniques with low transmitting power requirements and radiation shielding are needed to protect the crews and electronic equipment from radiation damage. Therefore, XCOM devices can be equipped as a supplementary system by Mars probes and used as a high-speed emergency communication method during dust storms.

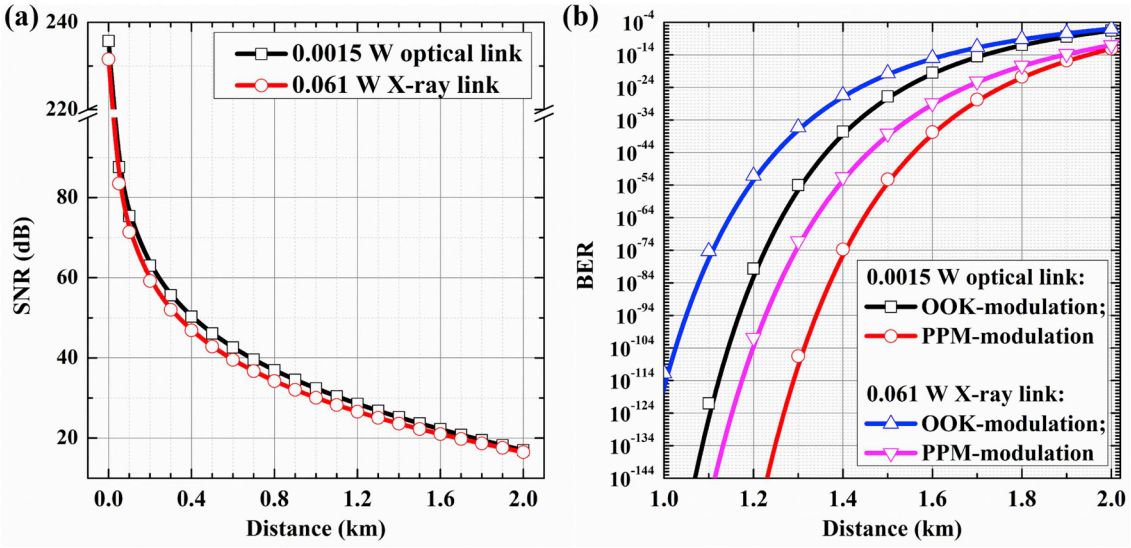

Fig. 15. (a) SNR and (b) BER of the communication link between the rovers as a function of the communication distance.

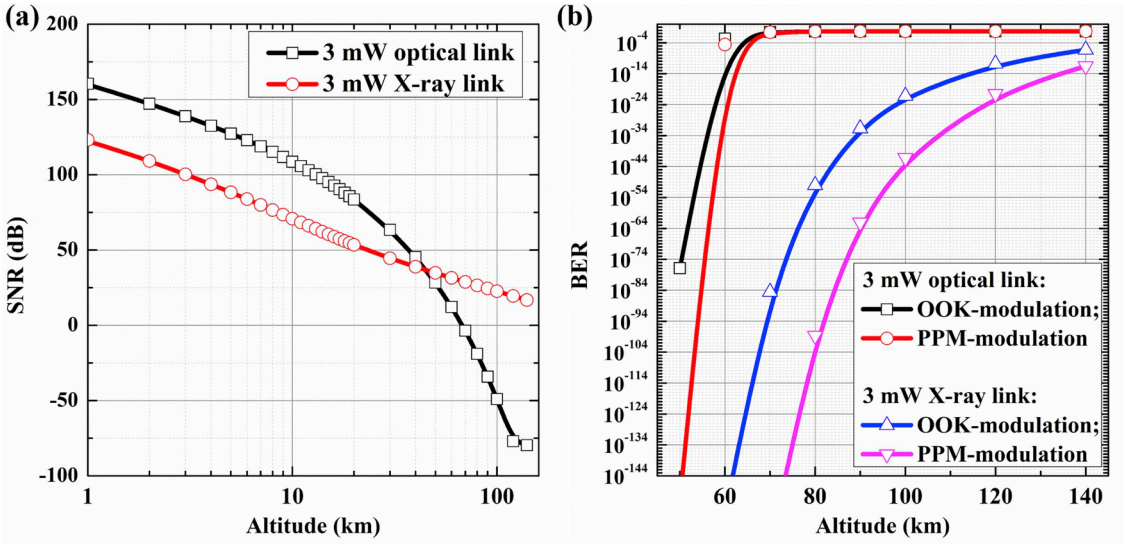

Fig. 16. (a) SNR and (b) BER of the communication link from the rover to the orbiter as a function of the altitude.

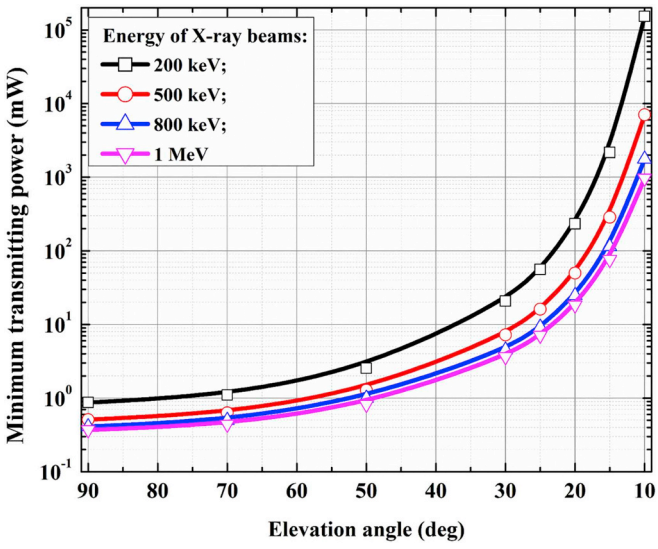

Fig. 17. Minimum transmitting power required for low-BER XCOM link with varying elevation angles.

Declaration of competing interest

None.

Acknowledgements

This work was supported by China Postdoctoral Science Foundation [Grant No. 2016M601807], the Fundamental Research Funds for the Central Universities [Grant No. NP2018408], the Fundamental Research Funds for the Central Universities [Grant No. NT2018017], the Fundamental Research Funds for the Central Universities [Grant No. NP2019410], the Postgraduate Research & Practice Innovation Program of Jiangsu Province [Grant No. KYCX18_0271], the General Technology and Field Fund for Equipment Pre-research [Grant No. JZX7Y20190258057701], the State Key Laboratory of Simulation and Effects of Intense Pulse Radiation Environment [Grant No. SKLIPR1813], the Special Foundation of China Postdoctoral Science Foundation [Grant No. 2018T110500], and the Nanjing University of Aeronautics and Astronautics PhD Short-term Visiting Scholar Project [Grant No. 190406DF06].

References

[1] J.M. Salotti, R. Heidmann, Roadmap to a human Mars mission, Acta Astronaut. 104 (2014) 558–564, https://doi.org/10.1016/j.actaastro.2014.06.038.

[2] Y. Wei, Z. Yao, W. Wan, China's roadmap for planetary exploration, Nat. Astron. 2 (2018) 346, https://doi.org/10.1038/s41550-018-0456-6.

[3] W. Farr, Technology development for high efficiency optical communications, IEEE Aerospace Conference, 2012, pp. 1–8, , https://doi.org/10.1109/AERO.2012.6187270.

[4] D.M. Boroson, A. Biswas, B.L. Edwards, MLCD: overview of NASA's Mars laser communications demonstration system, Proc. SPIE 5338 (2004) 16–29, https://doi.org/10.1117/12.543014.

[5] M. Taraba, K. Zwintz, C. Bombardelli, J. Lasue, P. Rogler, V. Ruelle, M. Treffer, A. Valavanoglou, M. Van Quickelberghe, M. Walpole, L. Wessels, Project M3—a study for a manned Mars mission in 2031, Acta Astronaut. 58 (2006) 88–104, https://doi.org/10.1016/j.actaastro.2005.04.013.

[6] D.S. Colburn, J.B. Pollack, R.M. Haberle, Diurnal variations in optical depth at Mars, Icarus 79 (1989) 159–189, https://doi.org/10.1016/0019-1035(89)90114-0.

[7] R. Greeley, P.L. Whelley, R.E. Arvidson, N.A. Cabrol, D.J. Foley, B.J. Franklin, P.G. Geissler, M.P. Golombek, R.O. Kuzmin, G.A. Landis, M.T. Lemmon, L.D.V. Neakrase, S.W. Squyres, S.D. Thompson, Active dust devils in Gusev crater, Mars: observations from the Mars exploration rover spirit, J. Geophys. Res.: Planets. 111 (2006) 1–16, https://doi.org/10.1029/2006JE002743.

[8] R.W. Zurek, L.J. Martin, Interannual variability of planet-encircling dust storms on Mars, J. Geophys. Res.: Planets. 98 (1993) 3247–3259, https://doi.org/10.1029/92je02936.

[9] G. Porter, See straight through data center bandwidth Limitations with X-ray, Tiny Trans. Comput. Sci. 2 (2013).

[10] NASA Technology Roadmaps, Communication, Navigation, and Orbital Debris Tracking and Characterization Systems, (2015) https://www.nasa.gov/sites/default/files/atoms/files/2015_nasa_technology_roadmaps_ta_5_communication_and_navigation_final.pdf , Accessed date: 10 January 2019.

[11] From NASA Goddard Space Flight Center, NASA Set to Demonstrate X-Ray Communications in Space, (2019) https://sciencesprings.wordpress.com/2019/02/20/from-nasa-goddard-space-flight-center-nasa-set-to-demonstrate-x-ray-communications-in-space/ , Accessed date: 26 September 2019.

[12] T. Su, Y. Li, L.Z. Sheng, P.F. Qing, C. Chen, N. Xu, B.S. Zhao, Space X-ray communication link modeling and power analysis, Acta Photonica Sin. 46 (2017), https://doi.org/10.3788/gzxb20174610.1035001 1035001-1.

[13] S. Hang, Y.P. Liu, H. Li, X.B. Tang, D. Chen, Temporal characteristic analysis of laser-modulated pulsed X-ray source for space X-ray communication, Nucl. Instrum. Methods Phys. Res., Sect. A 887 (2018) 18–26, https://doi.org/10.1016/j.nima.2018.01.031.

[14] G.A. Timofeev, N.N. Potrakhov, A.I. Nechaev, Experimental research of the X-ray communication system, Am. Inst. Phys. Conf. Proc. 2089 (2019) 020020, , https://doi.org/10.1063/1.5095749.

[15] S. Hang, X.B. Tang, H. Li, Y.P. Liu, J.X. Mu, W. Zhou, Novel approach for Mars entry blackout elimination based on X-Ray communication, J. Spacecr. Rocket. 56 (2019) 1–7, https://doi.org/10.2514/1.A34421.

[16] Y.P. Liu, H. Li, Y.L. Li, S. Hang, X.B. Tang, Transmission properties and physical mechanisms of X-ray communication for blackout mitigation during spacecraft re-entry, Phys. Plasmas 24 (11) (2017) 113507, , https://doi.org/10.1063/1.4998786.

[17] G.A. Landis, Dust obscuration of Mars solar arrays, Acta Astronaut. 38 (1996) 885–891, https://doi.org/10.1016/S0094-5765(96)00088-4.

[18] C.I. Calle, C.R. Buhler, M.R. Johansen, M.D. Hogue, S.J. Snyder, Active dust control and mitigation technology for lunar and Martian exploration, Acta Astronaut. 69 (2011) 1082–1088, https://doi.org/10.1016/j.actaastro.2011.06.010.

[19] MCD, Mars Climate Database, Software Package, (2018) Ver. 5.3 http://www-mars.lmd.jussieu.fr/mars/access.html , Accessed date: 10 January 2019.

[20] J.B. Madeleine, F. Forget, E. Millour, L. Montabone, M.J. Wolff, Revisiting the radiative impact of dust on Mars using the LMD global climate model, J. Geophys. Res.: Planets. 116 (2011) E11, https://doi.org/10.1029/2011JE003855.

[21] M.R. Balme, P.L. Whelley, R. Greeley, Mars: dust devil track survey in argyre planitia and hellas basin, J. Geophys. Res.: Planets. 108 (2003) E8, https://doi.org/10.1029/2003je002096.

[22] H. Wang, M.I. Richardson, R.J. Wilson, A.P. Ingersoll, A.D. Toigo, R.W. Zurek, Cyclones, tides, and the origin of a cross-equatorial dust storm on Mars, Geophys. Res. Lett. 30 (2003), https://doi.org/10.1029/2002gl016828.

[23] Mars 2020, Scientists Shortlist Three Landing Sites for Mars 2020, (2018) https://www.nasa.gov/feature/jpl/scientists-shortlist-three-landing-sites-for-mars-2020 , Accessed date: 10 January 2019.

[24] A.A. Fedorova, F. Montmessin, A.V. Rodin, O.I. Korablev, A. Määttänen, L. Maltagliati, J.L. Bertaux, Evidence for a bimodal size distribution for the suspended aerosol particles on Mars, Icarus 231 (2014) 239–260, https://doi.org/10.1016/j.icarus.2013.12.015.

[25] F. Forget, F. Hourdin, R. Fournier, C. Hourdin, O. Talagrand, M. Collins, J.P. Huot, Improved general circulation models of the Martian atmosphere from the surface to above 80 km, J. Geophys. Res.: Planets. 104 (1999) 24155–24175, https://doi.org/10.1029/1999je001025.

[26] E. Millour, F. Forget, A. Spiga, T. Navarro, J.B. Madeleine, L. Montabone, M.A. Lopez-Valverde, The Mars climate database (MCD version 5.2), European Planetary Science Congress, 10 2015, pp. 2015–2438.

[27] L. Montabone, F. Forget, E. Millour, R.J. Wilson, S.R. Lewis, B. Cantor, D. Kass, A. Kleinböhl, M.T. Lemmon, M.D. Smith, M.J. Wolff, Eight-year climatology of dust optical depth on Mars, Icarus 251 (2015) 65–95, https://doi.org/10.1016/j.icarus.2014.12.034.

[28] MCNP5/MCNPX, RSICC CODE Package CCC-740, (2008) https://rsicc.ornl.gov/codes/ccc/ccc7/ccc-740.html , Accessed date: 10 January 2019.

[29] J.A. Hoffman, M. Tarczon, B.T. Draine, GGADT: generalized Geometry anomalous diffraction theory, Extremes 7 (2) (2004) 179–190, https://doi.org/10.1007/s10687-005-6199-7.

[30] O.I. Korablev, V.A. Krasnopolsky, A.V. Rodin, E. Chassefiere, Vertical structure of Martian dust measured by solar infrared occultations from the PHOBOS spacecraft, Icarus 102 (1993) 76–87, https://doi.org/10.1006/icar.1993.1033.

[31] H. Weichel, Laser Beam Propagation in the Atmosphere, SPIE press, Washington, 1990.

[32] H.Q. Wang, Y. Yao, M.H. Gao, Transmission characteristics of laser signal in sand and dust weather, Chin. J. Lumin. 38 (2017) 522–529, https://doi.org/10.3788/fgxb20173804.0521.

[33] J.M. Chen, R.H. Mao, L.Y. Zhang, R.Y. Zhu, Large size LSO and LYSO crystals for future high energy physics experiments, IEEE Trans. Nucl. Sci. 54 (2007) 718–724, https://doi.org/10.1109/TNS.2007.897823.

[34] L. Pidol, A. Kahn-Harari, B. Viana, E. Vire, B. Ferrand, P. Dorenbos, J.T.M. de Haas, C.W.E. van Eijk, High efficiency of lutetium silicate scintillators, Ce-doped LPS, and LYSO crystals, IEEE Trans. Nucl. Sci. 51 (2004) 1084–1087 https://doi.org/10.4028/www.scientific.net/MSF.555.371.

[35] D. Liu, P.F. Qiang, L.S. Li, T. Su, L.Z. Sheng, Y.A. Liu, B.S. Zhao, X-ray focusing optics and its application in X-ray communication system, Acta Phys. Sin. 65 (2016) 010703, , https://doi.org/10.7498/aps.65.010703.

[36] Y.F. Yang, J.H. Qin, Z.L. Wang, Influence of Martian dust aerosol on laser transmission characteristics, Acta Photonica Sin. 47 (2018), https://doi.org/10.3788/gzxb20184703.0329001 0329001-006.

[37] D.N. Amanor, W.W. Edmonson, F. Afghah, Intersatellite communication system based on visible light, IEEE Trans. Aerosp. Electron. Syst. 54 (2018) 2888–2899, https://doi.org/10.1109/TAES.2018.2832938.

[38] E. Wei, S. Jin, Q. Zhang, J. Liu, X. Li, W. Yan, Autonomous navigation of Mars probe using X-ray pulsars: modeling and results, Adv. Space Res. 51 (2013) 849–857, https://doi.org/10.1016/j.asr.2012.10.009.

[39] Hamamatsu Photonics, Si APD S3884, (2018) https://www.hamamatsu.com/eu/en/product/type/S3884/index.html , Accessed date: 15 July 2019.

Shuang Hang received his BEng degree in nuclear engineering and nuclear technology from the University of South China, in 2013. He is a MD-PhD candidate in nuclear technology and materials engineering at Nanjing University of Aeronautics and Astronautics. His research interests are currently focused on modulated X-ray source, blackout communication and space laser/X-ray coupled communication technology.

Xiaobin Tang received his BEng degree in materials science and engineering from Nanjing University of Aeronautics and Astronautics, in 2000. He received his PhD degree in measuring and testing technologies and instruments from the same university, in 2009. He is now a professor in Department of Nuclear Science and Engineering at Nanjing University of Aeronautics and Astronautics. Tang' research interests include radiation energy conversion mechanism and nuclear battery technology, material irradiation effect and new materials for nuclear use, new technique and dose effect of radiation therapy, radiation detection and nuclear instrument development, and space radiation physics and nuclear technology application.

Huan Li received his BSc degree in physics from Northwest Normal University in 2012. He worked at the Institute of Modern Physics, Chinese Academy of Sciences from 2012 to 2014, engaging in particle accelerator research. Since then, Huan is a MD-PhD candidate at Nanjing University of Aeronautics and Astronautics, majoring in nuclear technology and materials engineering. His research interests are modulated X-ray sources based on laser-plasma interactions, blackout communication and laser/X-ray coupled communication technology.

Yunpeng Liu received his BSc degree in applied physics from Nanjing University of Aeronautics and Astronautics, in 2009. He received his PhD degree in nuclear technology and materials engineering from the same university, in 2014. He is currently working at Department of Nuclear Science and Engineering at Nanjing University of Aeronautics and Astronautics as an associate professor. His current research interests are application of Monte Carlo method in particle transport, design and preparation of new isotope battery, and space laser/X-ray coupled communication technology.

Junxu Mu received the BEng degree in radiation protection and nuclear safety from Nanjing University of Aeronautics and Astronautics, in 2017. He is master candidate in nuclear technology and application at Nanjing University of Aeronautics and Astronautics. His research interest is currently focused on pulsed X-ray detection technology.

Wei Zhou received the BEng degree in Physic from the Jiangxi Normal University, in 2015. He is master candidate studied in materials science and technology at Nanjing University of Aeronautics and Astronautics. His research interest is currently focused on the modulation techniques for X-ray communication.

Dang Peng received the BEng degree in nuclear engineering and nuclear technology from Nanjing University of Aeronautics and Astronautics in 2018. He is a master candidate in nuclear technology and application at Nanjing University of Aeronautics and Astronautics. His research direction is pulsed X-ray detection technology.

Sheng Lai received the BEng degree in Radiation Protection and Nuclear Safety from Nanjing University of Aeronautics and Astronautics, in 2018. He is a Master Candidate in nuclear technology and application at Nanjing University of Aeronautics and Astronautics. His research interest in plasma stealth technology and X-Rays communication.